

EFFECT OF PULSE SHAPE ON THE EFFICIENCY OF MULTIPHOTON PROCESSES: IMPLICATIONS FOR BIOLOGICAL MICROSCOPY

Christopher J. Bardeen,[†] Vladislav V. Yakovlev,[†] Jeff A. Squier,[‡] Kent R. Wilson,[†] Scott D. Carpenter,^{*} and Peter M. Weber^{**}

University of California, San Diego, [†]Department of Chemistry and Biochemistry and [‡]Department of Electrical and Computer Engineering, La Jolla, California 93093-0339; Brown University,

^{*}Department of Physics and ^{**}Department of Chemistry, Providence, Rhode Island 02912

(Paper JBO-209 received July 14, 1998; revised manuscript received Apr. 7, 1999; accepted for publication Apr. 8, 1999.)

ABSTRACT

The effects of spectral shape on two photon fluorescence excitation are investigated experimentally using an acousto-optic pulse shaper to modify femtosecond pulses from a Ti:sapphire laser. By using different spectral window shapes, we find that the measured two photon efficiency can vary by a factor of 2 for differently shaped spectra with the same full width at half maximum. We find that these effects are described well by a simple model assuming transform-limited pulses. The fact that even small changes in the spectral wings can significantly affect the efficiency of nonlinear processes has implications for biological multiphoton imaging, where it may be desirable to minimize sample exposure to radiation and maximize fluorescence or harmonic efficiency. © 1999 Society of Photo-Optical Instrumentation Engineers. [S1083-3668(99)00303-1]

Keywords two photon fluorescence; pulse shaping; multiphoton microscopy.

1 INTRODUCTION

To date, the primary laser variables in multiphoton microscopy used to optimize efficiency have been wavelength, average power, and peak power.¹⁻³ In this article we introduce a fourth parameter—the pulse shape. The temporal structure of the electric field which drives the multiphoton process depends on both the spectral amplitude and the phase. The spectral amplitude distribution, i.e., the power spectrum, determines the distribution of frequencies that make up the pulse, and the shortest, most intense pulse is obtained when these frequencies are all in phase and arrive at the same time. Both the spectral phase and the amplitude in the frequency domain determine, via Fourier transformation, the peak intensity and duration of the pulse in the time domain.⁴ An exact knowledge of these properties is crucial for estimating quantities like excitation cross sections and damage thresholds. Because the pulse shape is usually assumed to be a simple analytical form, such as a Gaussian or hyperbolic secant squared (sech^2), this means that the stated peak power, and consequently the intensity

at focus, has been based on certain assumptions. Thus, knowledge of the actual pulse shape is not only useful for maximizing the efficiency of the excitation, but is also *necessary* for an exact description of the fields generated at the focus. This will be critical in determining the optimal conditions for useful imaging and minimal biological damage.

A simple example using analytical shapes can be used to illustrate the importance of pulse shape. The time-bandwidth product of a pulse, defined as the full width at half maximum (FWHM) of the intensity profile of the pulse in the time domain ($\Delta\tau$), multiplied by the FWHM of its intensity profile in the frequency domain (i.e., the FWHM of the power spectrum, $\Delta\nu$) provides an indication of how the spectral content translates into the time domain. Consider the difference between a Gaussian pulse and a sech^2 pulse shape which have time-bandwidth products ($\Delta\nu\Delta\tau$) of 0.44 and 0.32, respectively. This belongs to an important class of pulse shapes, because self-mode-locked Ti:sapphire lasers, which are the most common lasers used in multiphoton microscopy, normally produce a time-bandwidth product that varies over this range. If we consider the case where the FWHM of the power spectrum, $\Delta\nu$, is identical for the two pulse shapes, we find that the Gaussian pulse shape produces a pulse that is 1.375 times longer (FWHM) in the time domain than the equivalent sech^2 pulse. If

The present address of Christopher J. Bardeen is Box 20-6, CLSL, Department of Chemistry, University of Illinois, 600 S. Mathews Ave., Urbana, IL 61801.

The present address of Vladislav V. Yakovlev is Department of Physics, University of Wisconsin, Milwaukee, Physics Building, P.O. Box 413, Milwaukee, WI 53201.

Address all correspondence to Dr. Jeff A. Squier: jsquier@sdchemw1.ucsd.edu

both pulses have the same total energy, then the peak intensity of the sech^2 pulse is greater and the probability of two photon absorption (2PA) increases proportionately, i.e., we expect the sech^2 pulse to generate a signal which is roughly 1.375 times stronger in two photon processes like second harmonic generation (SHG) and two photon absorption (2PA). The effect in third harmonic generation^{5,6} or three photon absorption^{7,8} is even more dramatic—the shorter sech^2 pulse should enhance the signal by almost a factor of 2. The difference between a Gaussian and a sech^2 spectrum with the same $\Delta\nu$ lies mainly in the low amplitude wings and may not be readily apparent to the casual observer. This example illustrates how relatively small changes in the frequency domain can lead to significant effects in the time domain and in the yields of multiphoton processes driven by these short pulses.

It is worth noting that this information is also useful for designing a multiphoton laser system.⁹ For example, recently available mode-locked fiber laser systems inherently work in the soliton regime, and thus tend to produce pulses with time bandwidth products on the order of 0.32. Thus this type of laser source should result in more efficient multiphoton imaging. Even if the spectrum from the laser itself is fixed, the optics in the system may affect the laser spectrum seen by the sample. For instance, if the passive optical components used in many fluorescence imaging experiments have limited bandwidths, they can act as spectral filters and may affect the pulse shape at the experiment.

Since experimental laser spectra rarely achieve ideal Gaussian or sech^2 profiles, it is worth exploring experimentally the effect of spectral shape on the efficiency of the 2PA process. Femtosecond pulse shaping has been used previously to optimize both second harmonic generation^{10,11} and one photon fluorescence.¹² In the present work, we use a femtosecond pulse shaping apparatus^{12,13} to controllably modify the spectral amplitude of femtosecond Ti:sapphire pulses and then use these shaped pulses to excite two photon fluorescence from dye molecules in solution or to generate second harmonic in a nonlinear crystal. In both cases, we vary both the bandwidth and the detailed spectral shape. We find that both processes are quite sensitive to the detailed shape of the spectrum, especially to the presence of low-amplitude wings. A simple model, based on assuming an instantaneous, frequency-independent nonlinearity, gives good agreement with the experimental data. The implications of this work are that the details of the temporal profile of the pulse, as deduced from the Fourier transform of its frequency spectrum, do not get washed out in a real 2PA experiment and can change the measured two photon efficiency (2PE), defined as the fluorescence output divided by the square of the pulse energy, by a factor of 2 or more.

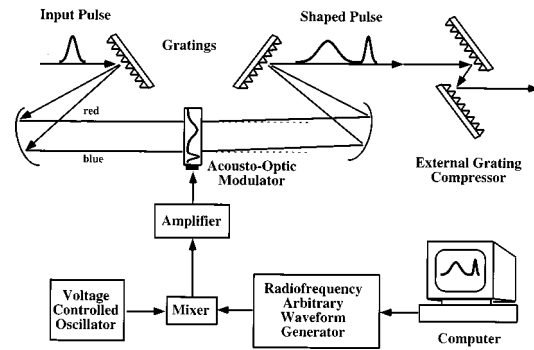


Fig. 1 Schematic of the computer controlled acousto-optic modulator pulse shaping system.

This clearly illustrates that simplistic assumptions of Gaussian or sech^2 pulse shapes are insufficient to determine the maximum achievable 2PE of a given laser system, and that the detailed spectral shape must be taken into account.

2 EXPERIMENT

To produce the input pulses for the pulse shaper, the output of a Ti:sapphire oscillator travels through a grating stretcher and then seeds a regenerative amplifier operating at a 1 kHz repetition rate. A birefringent filter in the amplifier cavity provides a wavelength-dependent loss which prevents the gain narrowing usually associated with regenerative amplification.¹⁴ This pulse is further amplified in a two pass postamplifier before passing through a grating compressor. The input laser pulse spectrum typically has a bandwidth of 800 cm^{-1} and a duration of about 45 fs, limited by residual cubic phase distortion. Our pulse shaper, shown in Figure 1, is based on the design of Warren and co-workers¹³ using an acousto-optic modulator (AOM). Briefly, the input beam, 1 cm in diameter, is dispersed in frequency by a 1200 line/mm grating and focused onto a TeO_2 acousto-optic crystal using a 0.5 m focal length spherical mirror. In the crystal, the optical wave is mixed with an acoustic wave generated by a radio-frequency (rf) pulse coupled into the crystal by a transducer. We use high power (1.5 W peak power) rf pulses in order to improve the diffraction efficiency of the AOM. The acousto-optic effect results in a diffracted optical wave proportional to the product of the two incident waves. The diffracted beam is recollimated and reassembled in frequency by a second spherical mirror and the grating. An external grating pair is used to compensate for the large linear chirp introduced by the diffraction of the AOM. Using a large diameter beam and limiting the amount of AO modulation help to minimize the temporal walkoff effects inherent in these spectral pulse shaping schemes,^{15,16} and we do not observe any spatial distortion in the shaped beam profile.

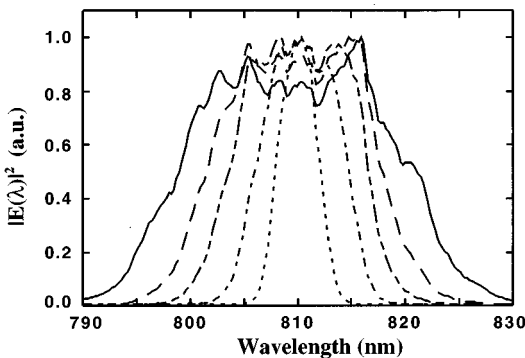


Fig. 2 Series of output power spectra shaped using sech rf windows of increasing width. The short-dashed line represents the narrowest window which most closely resembles a true sech^2 spectrum.

In the AOM pulse shaping method, the rf wave form, $V_{\text{rf}}(t_{\text{rf}})$, is converted to a traveling acoustic wave in the modulator. For small optical bandwidths, the laser pulse is linearly dispersed in frequency at the modulator and thus different time slices of the rf wave form modulate different frequency components of the input laser pulse, $E_{\text{opt}}^{\text{in}}(\nu_{\text{opt}})$, according to the relation

$$E_{\text{opt}}^{\text{out}}(\nu_{\text{opt}}) \propto E_{\text{opt}}^{\text{in}}(\nu_{\text{opt}}) V_{\text{rf}}(t_{\text{rf}}). \quad (1)$$

By changing the shape of the rf window in the AOM, we change the shape of the diffracted spectrum. The rf windows used in these experiments consist of square, Gaussian, sech, exponential, and stretched exponential. The exact functional forms are

$$\left\{ \begin{array}{l} 0 \quad t < -\tau_{\text{sq}} \\ 1 \quad -\tau_{\text{sq}} \leq t \leq +\tau_{\text{sq}} \\ 0 \quad t > +\tau_{\text{sq}} \end{array} \right\} \quad (\text{square}), \quad (2)$$

$$\exp(-t^2/\tau_{\text{ga}}^2) \quad (\text{Gaussian}), \quad (3)$$

$$2/[\exp(t/\tau_{\text{se}}) + \exp(-t/\tau_{\text{se}})] \quad (\text{sech}), \quad (4)$$

$$\exp(-|t/\tau_{\text{ex}}|) \quad (\text{exponential}), \quad (5)$$

$$\exp(-\sqrt{|t/\tau_{\text{st}}|}) \quad (\text{stretched exponential}). \quad (6)$$

Note that the sech rf window results in a sech^2 intensity profile in the optical spectrum. If the input pulse had a perfectly flat and infinite spectrum, these windows would transfer their shape directly onto the optical spectrum. Instead, the output spectral amplitude is more complicated and does not have a simple functional form since the input spectrum has a nonideal shape. Figure 2 shows the measured power spectra resulting from using a series of sech rf windows with varying widths. We do not in general create a perfect sech^2 spectral intensity profile due to inhomogeneities in the input pulse spec-

trum and also due to nonlinear acoustic pulse propagation which distorts the rf pulse in the AOM. For the sake of brevity, we will refer to a pulse that has been windowed by a square rf wave form as a “square pulse,” even though the optical spectrum is not truly square. Nevertheless, the different rf windows do result in qualitatively different output pulse spectra, especially in the wings, and these differences will serve to illustrate the main points of this article.

The two photon experiments themselves are done in a solution of rhodamine 610 and methanol with a concentration of approximately 10^{-4} molar. The maximum pulse energy, with full spectrum, is about 100 nJ and the 5 mm diam beam is focused using a 38 mm focal length lens into a cuvette containing the dye solution. Assuming a Gaussian beam profile and diffraction limited focusing, these parameters would result in a maximum intensity in the sample of roughly 10^{12} W/cm². No nonlinear effects such as self-focusing or continuum generation were observed. The fluorescence is collected at an angle of 90° to the exciting beam by a photomultiplier tube equipped with a glass filter to reject scattered 800 nm photons. A fraction of the exciting beam is split off and monitored using a reference photodiode, so that the fluorescence and pulse energy are measured simultaneously. The exciting beam is chopped at a frequency of 211 Hz to enable the use of lock-in detection. The second harmonic measurements are done in a similar manner, except that a 20 cm lens focuses the beam onto a 100 μm thick potassium dihydrogen phosphate (KDP) crystal and the second harmonic is detected collinearly.

In order to simplify our analysis, we try to compensate for the spectral phase as well as possible. By using an external grating compressor we compress the full diffracted spectrum, i.e., the width of the rf window is set equal to the width of the rf crystal, and the output pulse is measured using noncollinear autocorrelation in a thin KDP crystal. The measured autocorrelation width is 88 fs, while the width of the autocorrelation calculated from the transform limit of the measured spectrum is 55 fs, which corresponds to an intensity FWHM of 43 fs for this spectrum. Thus the full spectrum is roughly a factor of 1.5 off the transform limit. This phase distortion is relatively small and its effect on the narrower shaped spectra we analyze should be even smaller.

3 RESULTS

The power dependence of the fluorescence due to the 2PA was measured for several different pulse shapes and was found to depend on the square of the pulse energy in all cases. Thus we can define the 2PE as the fluorescence signal divided by the square of the pulse energy, normalizing out any fluctuations in power. Figure 3 shows the 2PE as a function of the FWHM of the measured power

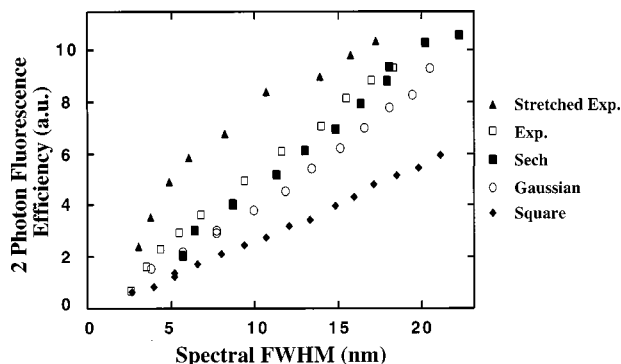


Fig. 3 The two photon fluorescence yield, defined as the fluorescence signal divided by the laser pulse energy squared, for five rf window shapes: square (\blacklozenge), Gaussian (\circ), sech (\blacksquare), exponential (\square), and stretched exponential (\blacktriangle). Note that the curves begin to converge at large FWHM values due to the limited extent of the input spectrum.

spectrum for several different pulse shapes. The ordinate is plotted in nanometers to facilitate comparison with easily measurable experimental quantities, and within this wavelength range $\Delta\lambda$ is proportional to $\Delta\nu$ to within 2%. The differences between pulse shapes is dramatic: from bandwidths of 3 to about 15 nm, a stretched exponential spectrum is almost three times as efficient as a square spectrum of the same FWHM. As expected from the discussion in Sec. 1, the difference between a sech² and a Gaussian spectrum is significant, even though the measured spectra look almost identical. Figure 4 shows representative Gaussian and sech² shaped spectra whose FWHMs are approximately 16 nm. The slight differences in the wings translate into a 12% difference in the 2PE, as can be seen in Figure 3. After FWHMs of about 15 nm, we begin to run out of the input spectrum and the efficiency of the stretched exponential pulse begins to level off. This is because the stretched exponential has the largest wings, and their extent is limited by the input bandwidth to the pulse shaper.

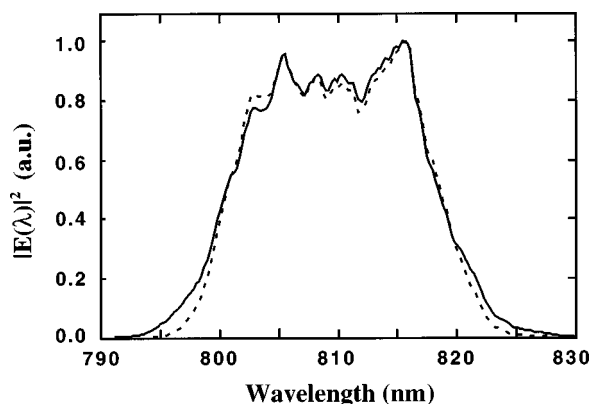


Fig. 4 Representative shaped spectra with spectral FWHMs of approximately 16 nm: using a sech rf window (solid line) and a Gaussian window (dashed line).

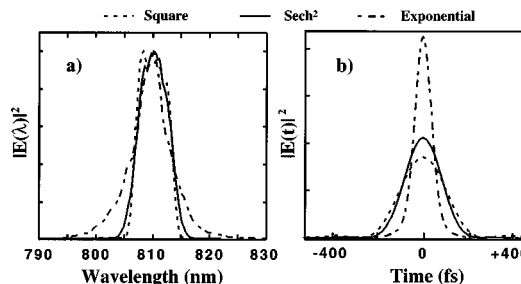


Fig. 5 (a) Representative power spectra with FWHMs of approximately 6.5 nm. The three types of rf windows used to generate the spectra are square (dashed line, FWHM=6.6 nm), sech² (solid line, FWHM=6.4 nm), and stretched exponential (short and long dashed lines, FWHM=6.1 nm). (b) Temporal intensity profiles of the Fourier transforms of the spectra in (a), normalized so that they have the same integrated area and thus the same pulse energy.

The other pulse shapes do not level off as quickly because they have smaller wings and at 15 nm FWHM they have not yet run into the limits of the input pulse spectrum. Also, for the narrowest spectral widths, the stretched exponential shows nonlinear behavior, most likely due to distortions of the shaped rf pulse in the acoustic crystal. Very similar curves are obtained for the efficiency of second harmonic generation, but those curves are not shown here. Finally, we note that, in both cases, the efficiency increases linearly with the FWHM in the sub-15 nm range, as expected for a two photon process.

We can analyze the effect of spectral shape on 2PE in more detail by considering the three representative spectra shown in Figure 5(a). These three spectra correspond to a FWHM of just over 6 nm and are the results of square, sech, and stretched exponential windows. Again, it is clear that none of the spectra is a true replica of the rf wave form, but they all possess important characteristics of those ideal spectra, especially in the shape of the wings. By assuming that the pulses are transform limited (i.e., there is no phase structure or chirp) and by Fourier transforming the square root of the power spectrum, we obtain $E(t)$. Taking the absolute value squared of this $E(t)$ results in $I(t)$, the calculated intensity profile. These are shown in Figure 5(b), normalized so that the integrated pulse energy is the same for all three shapes. The autocorrelation functions derived from these calculated $I(t)$'s reproduce the general shape and FWHM of the experimentally measured autocorrelations to within a few percent. We see that spectral wings in the frequency domain lead to an enhancement of the peak intensity in the time domain. Since any nonresonant multiphoton process depends nonlinearly on the pulse intensity, even a small enhancement can lead to large effects in the yield of the multiphoton process.

Although from the simple arguments presented in Sec. 1 we expect the relative 2PE of a pair of

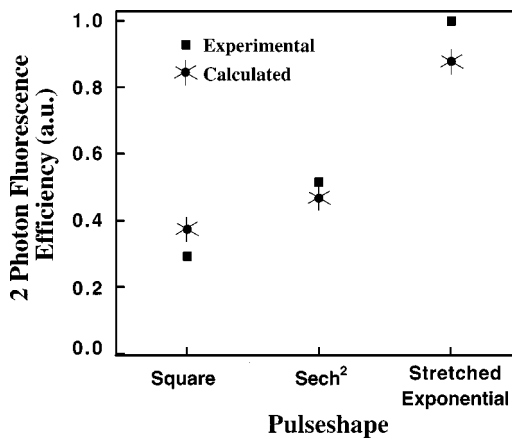


Fig. 6 Calculated and measured two photon fluorescence yields for the pulses in Fig. 5. The measured yields correspond to the measured power spectra in Fig. 5(a), while the calculated yields are derived from the intensity profiles in Fig. 5(b) and the equations in the text.

pulses to vary roughly as the ratio of their time durations, it is a simple matter to calculate the efficiencies explicitly. We make the simplifying assumptions that the absorption process is truly instantaneous and is independent of the wavelength, at least over our limited wavelength range. In this case, the total amount of 2PA (and thus fluorescence) is directly proportional to $\int_{-\infty}^{\infty} I(t)^2 dt$. The total pulse energy is proportional to $\int_{-\infty}^{\infty} I(t) dt$. Since the 2PE is defined as the fluorescence signal divided by the square of the pulse energy, we find that³

$$2 \text{ PE} \propto \frac{\int_{-\infty}^{\infty} I(t)^2 dt}{[\int_{-\infty}^{\infty} I(t) dt]^2}. \quad (7)$$

Using the calculated $I(t)$ in Figure 5(b), we can calculate the expected 2PE's and compare them with the experimentally measured values. Since Eq. (7) is not unitless and the absolute values of the two photon cross sections, spot size, etc. are not measured, we must scale the calculated yields by a constant value so they lie in the same range as the experimental values. The important point is that the calculated and experimental results shown in Figure 6 agree quite well, despite the assumptions inherent in our simple calculation of the 2PE. If anything, the calculation slightly underestimates the enhancement of the 2PE as we go from a square pulse to a stretched exponential. There are several possible reasons for this, the most likely being that an acoustic wave with sharp edges, like a square pulse, has a wider range of acoustic frequency components than a sech pulse of comparable FWHM. Thus the square acoustic wave will experience more distortion as it travels through the AO crystal and this could result in some phase distortion (chirp) on the shaped pulse. It is possible that the square pulse not only suffers from a lack of spectral

wings in the optical domain, but also may no longer be transform limited, which further decreases its peak intensity and thus its 2PE. Nevertheless, the simple calculation reproduces the variation in 2PE with respect to pulse shape almost quantitatively to within the experimental error, which is on the order of 5%. This very good agreement suggests that the contribution of any nonidealities, like residual chirp or distorted rf wave forms, is small. The fact that the spectral shape effect persists despite various nonidealities in the shaping and compression indicates that it is an experimentally robust variable.

4 DISCUSSION/CONCLUSION

It is widely recognized that to enhance the efficiency of a multiphoton process without resonant intermediate states, it is desirable to increase the average squared intensity at the sample. In general for a light field, $\Delta\nu\Delta\tau = \text{constant}$, where the constant depends on the details of the spectral shape. Given a specific spectral shape, one obvious way to shorten the pulse duration $\Delta\tau$ and increase the intensity is to increase $\Delta\nu$. Another method is to modify the spectral shape such that the constant (and thus $\Delta\tau$) becomes smaller. In this article we have emphasized that, even if the measured spectral FWHMs ($\Delta\nu$) are identical, adding a little amplitude in the spectral wings can change the pulse shape and result in significant 2PE enhancement. Small changes in the spectral shape, especially in the low amplitude wings, that are not taken into account by the crude measure of the FWHM, can have significant effects on the peak intensity and thus the 2PE. Such subtle changes in the spectral amplitude, such as that shown in Figure 4, can be introduced both by laser fluctuations and by passive optical elements like band pass filters. Equally important (although not emphasized in the present work) is the phase structure or chirp of the pulse spectrum.⁴ It is not sufficient to have a spectrally broad pulse—those spectral components must have the same phase. By adding spectral amplitude and removing spectral phase structure (chirp), we can make a pulse in which all the frequency components arrive simultaneously at the sample, resulting in the highest possible peak intensity and the most efficient multiphoton process. Other work in this group has shown how phase compensation of ultrashort, broad bandwidth pulses in microscope systems may be accomplished.¹⁷

We have recently developed multiple techniques which allow complete characterization of the temporal intensity and phase of the field at the focus of high numerical aperture systems.¹⁸ Thus, a pulse shape need no longer be assumed, and an accurate measure of the intensity and phase profiles is now possible. Consequently, for the first time, we can realistically consider the effects of the pulse amplitude and phase on the imaging process.

It is important to discover the optimum conditions for biological imaging using multiphoton excitation and fluorescence. The data and calculations presented in this article clearly illustrate the dangers of simplistic pulse shape analysis. Small differences between pulse shapes may be hardly noticeable in a linear measurement (e.g., the power spectrum), but can make a large difference in a nonlinear measurement (e.g., two photon absorption). Naive assumptions about the pulse shape, based on the measured FWHM of the power spectrum, can lead to differences of up to several hundred percent in the estimated 2PE. This work illustrates the necessity of accurate pulse characterization in order that exposure conditions in the sample be reproducible. This is especially true for studies relating to biological damage under multiphoton excitation.⁴ If the sample is sensitive to linear processes at the laser wavelength, like absorptive heating, then the key to maintaining sample viability during observation is to maximize the 2PE. Work by several groups¹⁹⁻²² has suggested that the main mechanism of biological damage at Ti:sapphire wavelengths is nonlinear rather than linear. In this case, it is doubtful that by maximizing the 2PE one can increase the useful imaging time, since one would also be maximizing the damage mechanisms. However, it is still necessary to characterize the exact intensity levels at which damage occurs in order to determine damage thresholds and optimum imaging conditions. Small changes in the wings of the pulse spectrum can produce significant changes in the peak intensity, and neglecting this consideration could result in a misinterpretation as to the exact intensity levels at which damage occurs. Thus, the details of pulse shape, both amplitude and phase, can have important implications for the practical application of multiphoton excitation of fluorescent or harmonic radiation for biological imaging.

REFERENCES

1. W. Denk, J. H. Strickler, and W. W. Webb, "Two-photon laser scanning fluorescence microscopy," *Science* **248**, 73-76 (1990).
2. W. Denk, "Two-photon scanning photochemical microscopy: Mapping ligand-gated ion channel distributions," *Proc. Natl. Acad. Sci. USA* **91**, 6629-6633 (1994).
3. C. Xu and W. W. Webb, "Measurement of two-photon excitation cross sections of molecular fluorophores with data from 690 to 1050 nm," *J. Opt. Soc. Am. B* **13**, 481-491 (1996).
4. W. Denk, D. W. Piston, and W. W. Webb, p. 445 in *Handbook of Biological Confocal Microscopy*, 2nd ed., J. B. Pawley, Ed., Plenum, New York (1995).
5. Y. Barad, H. Eisenberg, M. Horowitz, and Y. Silberberg, "Nonlinear scanning laser microscopy by third-harmonic generation," *Appl. Phys. Lett.* **70**, 922-924 (1997).
6. M. Muller, J. Squier, K. R. Wilson, and G. J. Brakenhoff, "3D-microscopy of transparent objects using third-harmonic generation," *J. Microsc.* **191**, 266-274 (1998).
7. M. Schrader, K. Bahlmann, and S. W. Hell, "Three-photon-excitation microscopy: Theory, experiment and applications," *Optik (Stuttgart)* **104**, 116-124 (1997).
8. H. K. Szmajcinski, I. Gryczynski, and J. R. Lakowicz, "Three-photon induced fluorescence of the calcium probe Indo-1," *Biophys. J.* **70**, 547-555 (1996).
9. D. L. Wosokin, V. Centonze, J. G. White, and D. Armstrong, "All-solid-state ultrafast lasers facilitate multiphoton excitation fluorescence imaging," *IEEE J. Sel. Top. Quantum Electron.* **2**, 1051-1065 (1996).
10. D. Yelin, D. Meshulach, and Y. Silberberg, "Adaptive femtosecond pulse compression," *Opt. Lett.* **22**, 1793-1795 (1997).
11. A. Efimov, M. D. Moores, N. M. Beach, J. L. Krause, and D. H. Reitze, *Opt. Lett.* **23**, 1915-1917 (1998).
12. C. J. Bardeen, V. V. Yakovlev, K. R. Wilson, S. D. Carpenter, P. M. Weber, and W. S. Warren, "Feedback quantum control of molecular electronic population transfer," *Chem. Phys. Lett.* **280**, 151-158 (1997).
13. C. W. Hillegas, J. X. Tull, D. Goswami, D. Strickland, and W. S. Warren, "Femtosecond laser pulse shaping by use of microsecond radio-frequency pulses," *Opt. Lett.* **19**, 737-739 (1994).
14. J. V. Rudd, G. Korn, S. Kane, J. Squier, and G. Mourou, "Regenerative amplification of 55-femtosecond pulses at a 1 kHz repetition rate: Model and experiment," *OSA Proc. Adv. Solid-State Lasers* **20**, 248-251 (1994).
15. M. A. Dugan, J. X. Tull, and W. S. Warren, "High-resolution acousto-optic shaping of unamplified and amplified femtosecond laser pulses," *J. Opt. Soc. Am. B* **14**, 2348-2358 (1997).
16. M. M. Wefers and K. A. Nelson, "Analysis of programmable ultrashort waveform generation using liquid-crystal spatial light modulators," *J. Opt. Soc. Am. B* **12**, 1343-1362 (1995).
17. M. Muller, J. Squier, R. Wolleschensky, U. Simon, and G. J. Brakenhoff, "Dispersion precompensation of 15 femtosecond optical pulses for high-numerical aperture objectives," *J. Microsc.* **191**, 141-150 (1998).
18. D. N. Fittinghoff, J. A. Squier, C. P. J. Barty, M. Muller, J. Sweetser, and R. Trebino, "Collinear type II second harmonic generation frequency resolved optical gating for use with high numerical aperture objectives," *Opt. Lett.* **23**, 1046-1048 (1998).
19. K. Konig, H. Liang, M. W. Berns, and B. J. Tromberg, "Cell damage by near-IR microbeams," *Nature (London)* **377**, 20-21 (1995).
20. K. Konig, H. Liang, M. W. Berns, and B. J. Tromberg, "Cell damage in near-infrared multimode optical traps as a result of multiphoton absorption," *Opt. Lett.* **21**, 1090-1092 (1996).
21. A. Schonle and S. W. Hell, "Heating by absorption in the focus of an objective lens," *Opt. Lett.* **23**, 325-327 (1998).
22. K. Konig, P. T. C. So, W. W. Mantulin, and E. Gratton, "Cellular response to near-infrared femtosecond laser pulses in two photon microscopes," *Opt. Lett.* **22**, 135-136 (1997).